Cell. Mol. Life Sci.
DOI 10.1007/s00018-008-8184-1

Cellular and Molecular Life Sciences

Research Article

Olfactory ensheathing cells are attracted to, and can endocytose, bacteria

J. Y. K. Leung[a], J. A. Chapman[b], J. A. Harris[a], D. Hale[a], R. S. Chung[a], A. K. West[a] and M. I. Chuah[a,*]

[a] Menzies Research Institute, University of Tasmania, Private Bag 24, Hobart, Tasmania 7001 (Australia), Fax: +61-3-62262679, e-mail: Inn.Chuah@utas.edu.au
[b] Discipline of Anatomy and Physiology, University of Tasmania, Hobart, Tasmania (Australia)

Received 8 April 2008; received after revision 23 June 2008; accepted 25 June 2008

Abstract. Olfactory ensheathing cells (OECs) have been shown previously to express Toll-like receptors and to respond to bacteria by translocating nuclear factor-κB from the cytoplasm to the nucleus. In this study, we show that OECs extended significantly more pseudopodia when they were exposed to *Escherichia coli* than in the absence of bacteria (p=0.019). Co-immunoprecipitation showed that *E. coli* binding to OECs was mediated by Toll-like receptor 4. LysoTracker, a fluorescent probe that accumulates selectively in lysosomes, and staining for type 1 lysosome-associated membrane proteins demonstrated that endocytosed FITC-conjugated *E. coli* were translocated to lysosomes. They appeared to be subsequently broken down, as shown by transmission electron microscopy. No obvious adherence to the membrane and less phagocytosis was observed when OECs were incubated with inert fluorescent microspheres. The ability of OECs to endocytose bacteria supports the notion that OECs play an innate immune function by protecting olfactory tissues from bacterial infection.

Keywords. Olfactory ensheathing cells, chemotaxis, endocytosis, innate immunity, ultrastructure.

Introduction

Life-threatening infections of the brain or meninges can occur *via* a number of routes, including invasion of bacteria from the bloodstream across the blood-brain barrier, by direct spread from the sinuses or middle ear, or by transport along peripheral nerves into the central nervous system (CNS) [1]. The olfactory nerves are one set of peripheral nerves along which bacteria can invade the CNS. Olfactory neurons possess dendrites that contact the air in the nasal cavity, where they detect odors but which also make them susceptible to airborne pathogens. The axons of olfactory neurons, which form the olfactory nerves, travel through the nasal mucosa, and then through the skull, to enter the olfactory bulbs, which are parts of the CNS [2]. Olfactory ensheathing cells (OECs), a specialized glial cell type, accompany the olfactory axons along their entire length throughout the periphery and the CNS [3].

In healthy individuals mechanisms that prevent pathogenic infections include sneezing and mucociliary clearance, the presence of cells of the innate and adaptive immune system in the nasal mucosa, and apoptotic cell death of infected olfactory neurons [4, 5]. In the unperturbed animal, small numbers of macrophages, assumed to be responsible for disposing of degenerating epithelial cells, are present in the olfactory epithelium of the nasal cavity. Their num-

* Corresponding author.

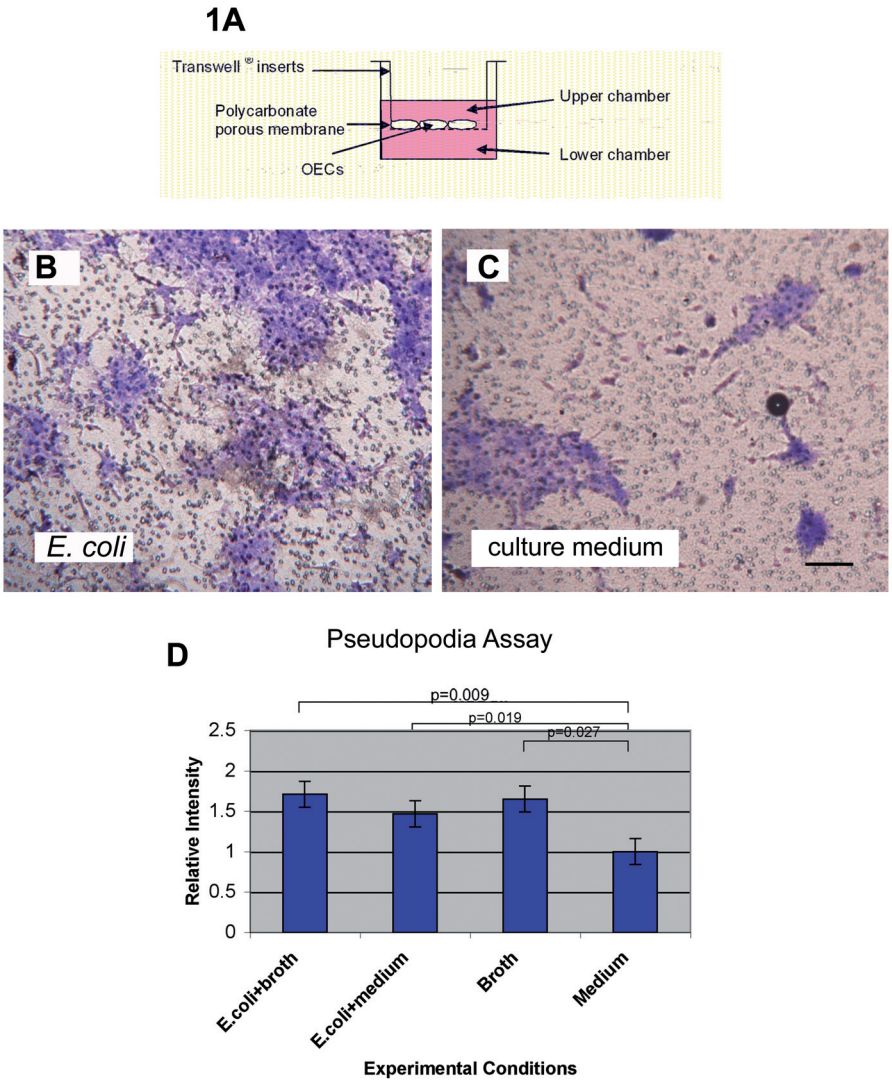

Figure 1. (*A*) Set-up of pseudopodia assay in which olfactory ensheathing cells (OECs) are seeded into inserts (upper chamber) and separated from the test solution in the lower chamber by a porous polycarbonate membrane. Presence of chemoattractive agent in the lower chamber induces the extension of pseudopodia through the pores and on to the lower surface of the membrane. (*B, C*) Cell bodies from inside the insert have been removed, and pseudopodia present on the under surface have been stained with crystal violet. With *E. coli* present in the lower chamber (*B*), more pseudopodia are visible compared to that in the absence of *E. coli* (*C*). The small specks distributed evenly throughout (*B*) and (*C*) are the pores of the insert. Scale bar = 100 μm in (*B*) and (*C*). The pseudopodia assay (*D*) shows that OECs extended significantly more pseudopodia through the pores of the insert when the culture medium contained *E. coli* (p=0.019) or *E. coli* and nutrient broth (p=0.009) than in the absence of *E. coli.* Inclusion in the culture medium of nutrient broth (which contained yeast extracts) was also associated with a significant increase in pseudopodia (p=0.027) relative to culture medium alone. Error bar = SEM.

bers are markedly increased in the aftermath of injury and infection by neurotropic pathogens that induce rapid and massive death of olfactory neurons. In addition, supporting cells of the olfactory epithelium also become phagocytic as indicated by the presence of phagosomes and apoptotic bodies in the cytoplasm [6].

In a recent study, we showed that a subset of OECs displayed nuclear localization of nuclear factor (NF)-κB, an inflammatory transcription factor, after treatment with *Escherichia coli* and lipopolysaccharide (LPS), a component of the cell walls of Gram-negative bacteria, such as *E. coli* [7]. Immunostaining for the chemokine Gro demonstrated a functional response that was consistent with NF-κB activation. Furthermore, OECs were shown to express Toll-like receptors 4 (TLR4), which bind and are activated by LPS. These findings demonstrate that OECs possess the cellular machinery that permits them to respond to certain bacterial ligands, and may have an innate immune function.

This study investigated further the innate immune function of OECs. We hypothesized that OECs are attracted to *E. coli* and can endocytose them subsequent to binding *via* TLR4. Here, using a pseudopodia assay, we show that OECs demonstrate chemotaxis towards *E. coli.* We also present evidence that OECs are capable of endocytosing *E. coli* using a fluorescent tracker for lysosomes and transmission electron microscopy.

Materials and methods

OEC and *E. coli* culture. All procedures conducted on animals were approved by the Animal Experimenta-

tion Ethics Committee of the University of Tasmania and are consistent with the Australian Code of Practice for the Care and Use of Animals for Scientific Purposes. Tissues for cell culture were harvested from 2-day-old Hooded Wistar rats, and cells were cultured in DMEM supplemented with 10 % (vol/vol) fetal calf serum (JRH Biosciences, Brooklyn, VIC, Australia) and 1 % (vol/vol) penicillin-streptomycin-amphotericin B solution (DMEM-10S; Sigma, St Louis, MO, USA). OECs were sourced from the olfactory mucosa and outer nerve layer of the bulb because together with the olfactory nerves, they constitute an uninterrupted cellular route between the external environment and the CNS. Briefly, olfactory mucosa and olfactory nerve layer were harvested, pooled, dissociated and cultured as previously described [8]. OECs were purified for 3 days in 100 μM cytosine-β-D-arabinofuranoside (Sigma) and expanded for 4 days in 100 μg/ml bovine pituitary extract (Sigma). OECs were identified by their positive staining for $p75^{NTR}$ using either rabbit anti-$p75^{NTR}$ (1:100) (Promega, Annandale, Australia) or mouse monoclonal anti-$p75^{NTR}$ (1:100) (Chemicon, Temecula, CA, USA) followed by goat anti-rabbit AlexaFluor 594 (1:1000) (Molecular Probes, Eugene, OR, USA) or goat anti-mouse AlexaFluor 488 (1:1000) (Molecular Probes), respectively. Nuclear staining was done by incubating with Hoechst S769121 (10 μg/ml) (Molecular Probes) for 5 min. Staining for CD11b showed that the cultures contained less than 1 % macrophages, and these cells did not express $p75^{NTR}$ (data not shown).

E. coli strain JM109 (Promega) was cultured overnight, killed by autoclaving and stored at –20°C in aliquots. Control broth was treated and stored in exactly the same way, except for the bacterial inoculation. *E. coli* or control broth was used at a 1:125 dilution. This equates to1.6×10^6 bacteria/well, according to the formula: 1 OD unit at 600 nm = 10^9 *E. coli* cells/ml [9]. For some pseudopodia assays, *E. coli* in broth were centrifuged, pellet washed free of broth (and yeast) and resuspended at the original density in culture medium.

Pseudopodia assay. The pseudopodia assay measured pseudopodia extending through pores in polycarbonate membrane Transwell® inserts (8-μm pore size, Corning, Acton, USA) that were placed into 12-well tissue culture plates (Fig. 1A). In the assay, 1.5 ml of culture medium was added to each well and 8500 OECs in 500 μl culture medium were plated into the porous insert in each well (upper chamber). Cells were allowed to adhere to the polycarbonate membrane for 48 h before 100 μl of test solution was added to the culture medium in the wells outside the inserts (lower chamber). Any molecular interactions between OECs and test solutions were therefore only possible *via* the pores in the inserts. The test solutions were: culture medium; broth; *E. coli* + culture medium; *E. coli* + broth. Pseudopodia were imaged and quantitated after 5-h incubations of OECs in the presence of test solutions.

To visualize pseudopodia that had extended through the pores, the upper surface of the insert bearing the cell bodies was wiped clean with a cotton swab. The membrane inserts were stained for 20 min with a solution of phosphate-buffered saline containing 0.7 % (wt/vol) crystal violet and 50 % (vol/vol) methanol, after which they were rinsed in distilled water for 5 min. This procedure stained the pseudopodia that had extended through the pores and were present on the under surface of the membrane insert. Membranes were then removed from inserts with a pair of scissors and mounted with D.P.X (Koch-Light Laboratories, Suffolk, UK) on a glass slide for viewing under an Olympus BX50 microscope.

For quantitative evaluation of pseudopodia formation, the quantitative pseudopodia kit (Chemicon) was used. This assay involved staining the pseudopodia, extracting the dye and determining the absorbance level. The absorbance level correlates directly with the extent of pseudopodia formation. The assay was performed according to the instructions of the manufacturer's kit. Briefly, the procedure for staining the pseudopodia is as described previously. The stained pseudopodia were incubated with the dye extraction buffer for 15 min and the absorbance of the extraction buffer was then measured at OD_{600} in a microplate reader (TECAN GENios, San Jose, CA, USA). To compensate for variability between experiments, the absorbance value corresponding to control culture medium (without *E. coli*) was standardized to 1 in each experiment and values of other test conditions were expressed relative to this. The results were analyzed using one-way analysis of variance and pairwise multiple comparisons using the Student-Newman-Keuls method.

Co-immunoprecipitation of LPS and TLR4. Confluent cultures of OECs in 25 cm^2 flasks were untreated or treated to 100 μl (10^8) *E. coli* overnight. The medium and unbound *E. coli* were then removed; OECs washed and lysed in 250 μl dilution buffer (DL) (20 mM Tris, pH 7.6, 400 mM NaCl, 7.5 mM $MgCl_2$, 0.2 mM EDTA, 1.0 mM dithiothreitol). Next, 250 μl final buffer (FB) (20 mM Tris, pH 7.6, 100 mM NaCl, 7.5 mM $MgCl_2$, 0.2 mM EDTA, 0.5 % Igepal, 10 % glycerol) was added and extracts were pre-cleared by adding 50 μl 50 % (wt/vol) protein A-Sepharose (GE HealthCare Bio-Sciences AB, Uppsala, Sweden) suspension made up in DL. The mixture was incu-

bated at 4°C with shaking for 1 h after which extracts were centrifuged at 13 000 g, 4°C for 5 min to pellet the Sepharose. The supernatant was removed and monoclonal antibody to *E. coli* LPS (2.5 μg; Abcam, Cambridge, UK) was added to the extracts and incubated for 1 h at 4°C with shaking. Next, 50 μl 50 % protein A-Sepharose in DL was added and the entire mixture incubated overnight at 4°C with shaking. The following day, the antibody-protein-bead solution was centrifuged at 13 000 *g* for 5 min, and the resulting pellet washed three times with 200 μL FB. The final pellet was resuspended in 15 μL Nu-Page LDS sample buffer, and SDS-PAGE and Western blotting were performed as described previously [10], using the Nu-Page system (Invitrogen) and 10 % Bis-Tris gels. For all Western blots, equal protein amounts (10 μl) were loaded for all samples. Membranes were probed with a rabbit anti-TLR4 antibody (1:1000; sc-10741, Santa Cruz Biotechnology) and goat anti-rabbit-HRP secondary antibody (1:1000; Dako). A control blot was incubated in the absence of the primary antibody.

Immunofluorescence and use of LysoTracker as a lysosomal probe. To obtain fluorescently labeled bacteria, 25 μL 1 mg/ml fluorescein 5-isothiocyanate (FITC) was added to 500 μL *E. coli* suspension and mixed at 37°C for 2 h. The solution was then centrifuged at 12 100 *g* for 1 min to remove excess FITC. This was repeated two more times and, after the final wash, the *E. coli* were suspended in 1 ml culture medium.

LysoTracker (Molecular Probes) is a red fluorescence probe that accumulates selectively in cellular compartments such as lysosomes, which have a low internal pH. We used this probe as well as immunostaining for type 1 lysosome-associated membrane proteins (LAMP-1) to determine whether *E. coli* internalized by OECs are translocated to lysosomes. OECs were replated on to 13-mm diameter coverslips. Upon reaching confluence, 100 μL FITC-labeled *E. coli* was added to each coverslip and allowed to incubate overnight. In control cultures, OECs were exposed to inert 1-μm microspheres at a concentration of 3.6×10^7 microspheres/well (FluoSpheres F8823, Molecular Probes). The following day cultures were either treated with 2.5 μl of 25 μM LysoTracker (2 h) or immunostained for LAMP-1 (1:200; Santa Cruz Biotech, CA, USA). For immunostaining, all cultures were fixed in 4 % paraformaldehyde prior to incubation with primary antibodies, which routinely included anti-$p75^{NTR}$ to positively identify OECs. Cells were viewed either on an Olympus BX50 or Leica DM LB2 fluorescence microscope.

Transmission electron microscopy. Confluent cultures of OECs in 25-cm^2 flasks were treated to 100 μL (10^8) *E. coli* or 1-μm microspheres overnight. The following day, cells were fixed in 2 % glutaraldehyde in 0.1 M sodium cacodylate buffer for 4 h at 4°C. Cells were then rinsed three times with 0.1 M sodium cacodylate buffer, scraped off from the flask and centrifuged at 13 000 *g*. They were then post-fixed in 1 % (wt/vol) osmium tetroxide in 0.1 M sodium cacodylate buffer for 20 min at 4°C, rinsed in buffer and stained in saturated uranyl acetate in 50 % (vol/vol) ethanol for 10 min. Next, specimens were dehydrated in a graded series of ethanol (70–100 %), cleared in propylene oxide and immersed overnight in a 1:4 mix of propylene oxide and Procure 812. Specimens were then transferred to BEEM capsules containing Procure 812 and incubated for 48 h at 60°C. Thin sections were cut and viewed on a Philips CM100 transmission electron microscope.

Results

OECs demonstrate pseudopodia extension in response to *E. coli*. Light microscopy observations following crystal violet staining showed that more violet-stained regions, representing pseudopodia, were present on the under surface of the membrane insert when OECs were exposed to *E. coli* than in their absence (Fig. 1B, C). This was confirmed by the pseudopodia assay which showed that, when *E. coli* were suspended in broth or culture medium in the lower chamber, significantly more pseudopodia were observed on the lower surface of the membrane compared to culture medium alone in the lower chamber ($p=0.009$, $p=0.019$, respectively) (Fig. 1). Interestingly, OECs also extended significantly more pseudopodia when tested with bacterial nutrient broth without *E. coli* ($p=0.027$) (Fig. 1D), possibly related to the presence of yeast extracts in the broth. Nevertheless, the chemotropic effect of *E. coli* on OECs was clearly verified by the maintenance of increased OEC pseudopodial extension towards *E. coli* resuspended in broth-free medium (Fig. 1D).

***E. coli* bind to TLR4 expressed on OECs and are subsequently endocytosed.** After 6-h incubation many of the FITC-conjugated *E. coli* were associated with the outer plasma membranes of the $p75^{NTR}$-expressing OECs (Fig. 2A). In contrast, contaminating cells, which did not stain for $p75^{NTR}$ in the cultures, had few *E. coli* associated with their plasma membranes. When OECs were incubated with FluoSpheres, the fluorescent microspheres appeared to distribute randomly on the surface of the cells with no preferential

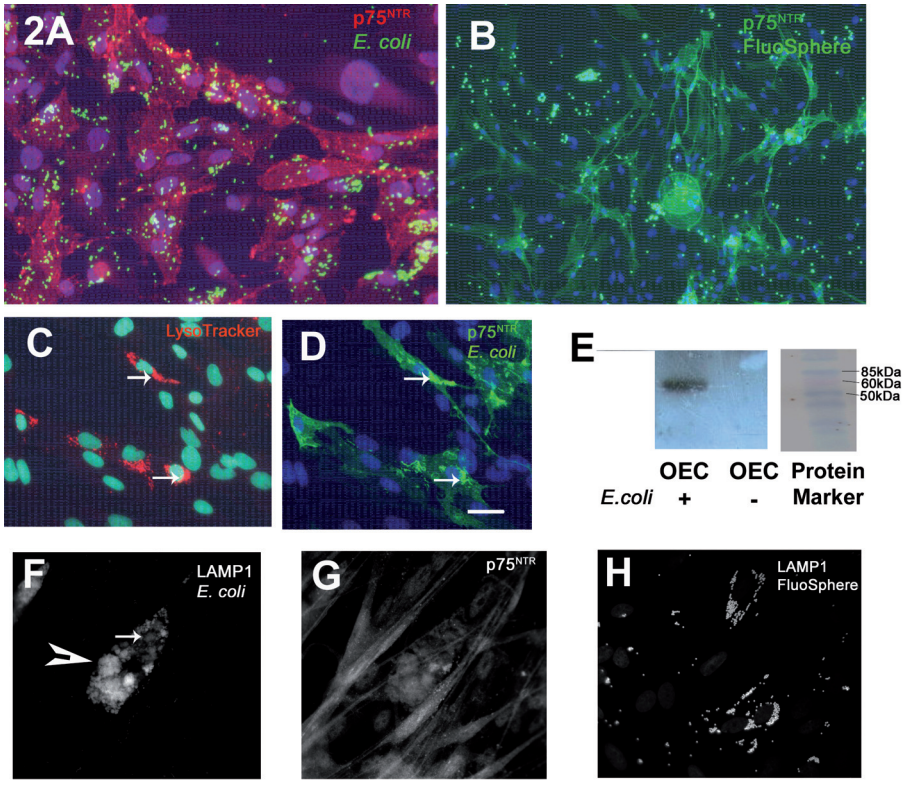

Figure 2. FITC-conjugated *E. coli* are associated preferentially with p75^{NTR}-positive (red) OECs (*A*) compared to fluorescent microspheres that are randomly dispersed both on p75^{NTR}-positive (green) OECs and cell-free regions of the glass coverslip (*B*). Following overnight incubation and the application of LysoTracker, some OECs demonstrate an increased formation of phagolysosomes (red spots, indicated by arrows in *C*), which colocalize with endocytosed FITC-conjugated *E. coli* (arrows in *D*). Endocytosis of *E. coli* is confirmed by positive staining of phagolysosomes with anti-LAMP-1(arrow in F), some of which contained large aggregates of *E. coli* that assumed the round profile of phagolysosomes (arrowhead in *F*). Cells were confirmed to be OECs by their positive staining for p75^{NTR} (*G*). OECs exposed to fluorescent microspheres rarely showed endocytosis and no detectable staining for LAMP-1 (*H*). Lysates prepared from OECs exposed to *E. coli* and untreated OECs (negative control) were incubated with anti-LPS. Immunoprecipitates were analyzed by Western blotting with anti-TLR4. Presence of band of the correct size (approximately 85 kDa) corresponding to OECs treated with *E. coli* confirms the binding of LPS in *E. coli* to TLR4 (*E*). Scale bar = 10 μm (*A*); 25 μm (*B*); 20 μm (*C, D, F–H*).

adhesion to p75^{NTR}-expressing OECs (Fig. 2B). Upon exposure to *E. coli* overnight, increased presence of phagolysosomes was observed in some OECs (Fig. 2C). In these cells, several fluorescent *E. coli* could be co-localized to the phagolysosomes, as indicated by the LysoTracker probe (Fig. 2D). This was also confirmed by double staining with anti-LAMP-1 and p75^{NTR} (Fig. 2F, G), which showed intracellular aggregates of *E. coli* that assumed a circular outline because they were sequestered in LAMP-1-positive lysosomes (arrowhead in Fig. 2F). OECs exposed to FluoSpheres rarely endocytosed the inert spheres and showed no detectable staining for LAMP-1 (Fig. 2H). In summary, these observations suggested that endocytosed *E. coli* may be subjected to digestion by lysosomal enzymes.

The co-immunoprecipitation results showed that the association of *E. coli* to OECs was due to LPS binding to TLR4 expressed on OECs, while OECs alone did not result in any bands (Fig. 2E). No band was observed in control blot incubated in the absence of the primary antibody (data not shown). Presence of band of the correct size (approximately 85 kDa) confirmed the binding of LPS in *E. coli* to TLR4.

Transmission electron microscopic observations demonstrated the contrast between the preferential association of *E. coli* with OEC plasma membranes (Fig. 3A, D) and the random distribution of inert microspheres (Fig. 3F). Some OECs that appeared to be actively phagocytosing bacteria possessed an uneven cell surface (Fig. 3C), which was not observed in OECs incubated with inert microspheres (Fig. 3F, G). In tangential sections that grazed the surface of OECs, phagosomes containing newly endocytosed *E. coli* were observed (Fig. 3B; asterisks). In the cytoplasm lysosomes could be identified by their morphology, either containing dense deposits or membrane whorls (Fig. 3C) [11, 12]. OECs that had fewer *E. coli* on their surface often possessed a large number of membrane-bound vesicles of variable electron density (Fig. 3D, E), suggesting that

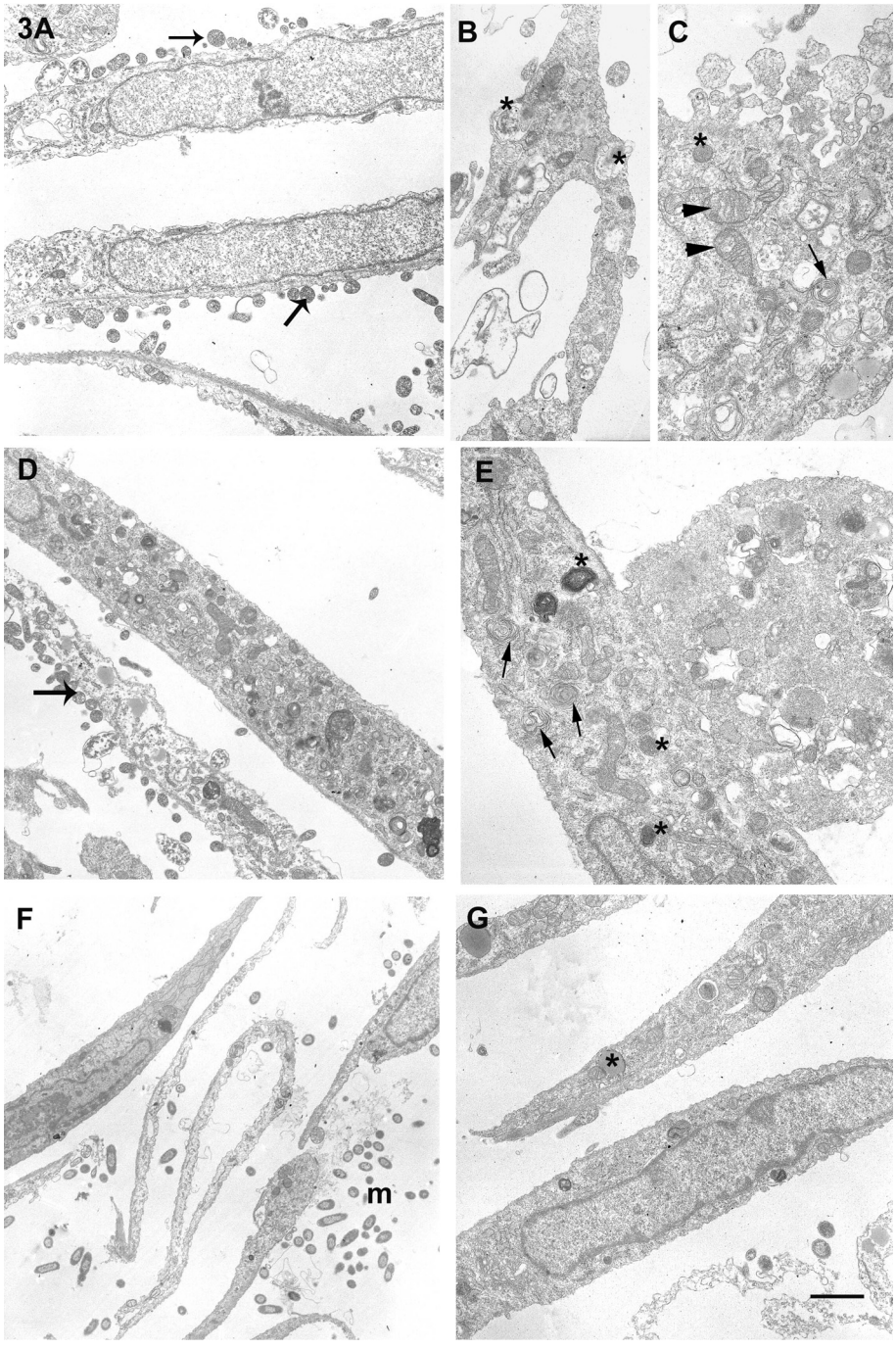

Figure 3. (*A–E*) OECs incubated with *E. coli*; (*F, G*) OECs incubated with microspheres. *E. coli* associate preferentially with OEC membrane (arrows, *A* and *D*). Some OECs have an uneven surface membrane (*B, C*), suggesting that they may be actively phagocytosing *E. coli.* In tangential sections, endocytosed *E. coli* were sequestered in phagosomes (* in *B*). At high magnification, lysosomes could be identified by their morphology, either containing dense deposits (* in *C*) or membrane whorls (arrows in *C, E*). Mitochondria could be distinguished from lysosomes generally by their elongated shape and the presence of cristae within (arrowheads in *C*). Olfactory ensheathing cells that had fewer *E. coli* on their surface often possessed a large number of membrane-bound vesicles of variable electron density (*D* and * in *E*). Inert microspheres (m) seeded on to OEC cultures did not show preferential association to OEC membrane (*F*). A small number of microspheres (* in *G*) were endocytosed by OECs, which generally had a smooth membrane surface. Scale bar = 1.2 μm (*A, D, F, G*), 0.5 μm (*B, C*), 0.6 μm (*D*).

they had endocytosed the *E. coli* that previously bound to their surface. The endocytosed *E. coli* appeared to be sequestered in phagolysosomes and were in various stages of breakdown. Although endocytosed microspheres were apparent in a few OECs, the lack of association between microspheres and OEC plasma membranes (Fig. 3F), the smooth surface of the OECs and the less frequently observed phagolysosomes (Fig. 3G) suggested that less phagocytic activity was induced by the microspheres than by *E. coli.*

Discussion

We show here for the first time that OECs are attracted to the Gram-negative bacteria *E. coli*, which

bind to TLR4 expressed on the OEC cell surface and are subsequently endocytosed, and possibly broken down by lysosomal enzymes. These findings have implications relating to OEC function as a key component of the primary olfactory pathway and their strategic location in the nasal cavity and in the olfactory bulb.

Extension of pseudopodia in OECs as they assume a migratory phenotype is most likely a common phenomenon during the normal ontogeny of the olfactory system. OECs originate from the olfactory placode and migrate with growing axons, but always ahead of the axon terminals as they project towards the olfactory bulb [13]. Thus in doing so, OECs effectively penetrate the transition zone between the periphery and CNS [14, 15]. It has been demonstrated that the directional cue for this migration may be due to soluble factors originating from the target tissue, the olfactory bulb [16]. Although the identity of olfactory bulb-derived factors has yet to be identified, a recent study showed that glial cell line-derived neurotrophic factor stimulates intercellular interaction of lamellipodial waves that contribute to OEC migration [17] and which may be critical for the establishment of olfactory axon projections between the nasal cavity and the brain.

The pseudopodia extension in response to *E. coli* observed in this study, and which precedes OEC migration, further supports the notion that OECs may have an innate immune function in addition to their widely accepted role as a guide for olfactory axons. In our previous study, we showed that incubation with *E. coli* triggered NF-κB translocation to the nucleus, accompanied by up-regulation of Gro1 in a subset of OECs [7]. Subsets of OECs were shown to express TLR4 both *in vitro* and *in vivo.* Although there is no report of OECs *in vivo* migrating free of axons in the lamina propria, and acting as immune surveillance cells, this scenario is plausible if extensive damage is inflicted on the olfactory epithelium. For example, when olfactory neurons and axons are induced to degenerate in the aftermath of intranasal irrigation with zinc sulfate, OECs are observed to migrate towards the basal part of the epithelium and the cribriform plate [18]. Most significantly, they were observed to participate in phagocytosis of cellular debris in the lamina propria [18, 19]. Phagocytosis of apoptotic cells during development as well as axonal fragments by OECs in culture have also been demonstrated [20, 21]. Whether or not OECs, under adverse conditions *in vivo*, can be activated to take on an immunological defensive role in addition to removing cellular debris remains to be investigated.

Although heat-treated *E. coli* were used in our study, the transmission electron microscopic observations, as indicated by the presence of phagolysosomes of variable densities, suggest that OECs have the capacity to eradicate live pathogens through precise biochemical mechanisms. This potential role is supported by the fact that OECs express antimicrobial peptides that are an evolutionarily conserved component of the innate immune system. Antimicrobial peptides contain domains of hydrophobic and cationic amino acids that are spatially arranged into an amphipathic design to facilitate their insertion into the bacterial membrane, ultimately resulting in membrane destabilization and bacterial lysis [22–24]. Two antimicrobial peptides known to be expressed in OECs are Neuropeptide Y (NPY) and lysozyme [8, 25, 26]. Neuropeptide Y is expressed in OECs of E15 rat embryos prior to the development of laminae in the olfactory bulb and it persists into adulthood [26]. It has been shown to have antifungal properties, *e.g.* against *Candida albicans* [27], and more recently against *E. coli* [28]. Lysozyme was originally identified in mucosal secretions and is present in Bowman's glands and OECs in the lamina propria of the olfactory region [8, 29]. It is bactericidal against both Gram-positive and Gram-negative bacteria through its ability to perturb bacterial membrane as well as its enzymatic function [30]. Another possible mechanism adopted by OECs is the production of nitric oxide [31]. We have preliminary *in vitro* data that show OECs up-regulate inducible nitric oxide synthase in response to *E. coli*, accompanied by increased presence of nitric oxide in the cytoplasm.

In summary, this study has shown that OECs demonstrate chemotaxis towards the Gram-negative bacteria, *E. coli*, which bind to TLR4 expressed on OECs. The ability of OECs to endocytose and dispose of bacteria has important implications for their postulated function as immune surveillance cells, particularly in situations where the nasal lining is compromised. In future studies we intend to assay the microbicidal activity of OECs during live bacterial challenges. In addition, the binding of LPS of *E. coli* with TLR4 raises the prospect of simultaneous phagocytosis of pathogens and activation of NF-κB [7], leading to cytokine up-regulation and adaptive immune system cell activation. These possibilities require investigation to gain a complete understanding of the immune capabilities of OECs.

Acknowledgment. This study was supported by a grant from the Institutional Research Grant Scheme (UTas) and the Royal Hobart Hospital Research Foundation.

1 Kielian, T. (2004) Immunopathogenesis of brain abscess. J. Neuroinflamm. 88, 454–461.
2 Chuah, M. I., Schwob, J. E. and Farbman, A. I. (2003) Developmental anatomy of the olfactory system. In: Hand-

book of Olfaction and Gustation, pp. 115–138, Doty, R. L. (ed.), Marcel Dekker, NY.
3 Chuah, M. I. and West, A. K. (2002) Cellular and molecular biology of ensheathing cells. Microsc. Res. Tech 58, 216–227.
4 Mori, I., Goshima, F., Imai, Y., Kohsaka, S., Sugiyama, T., Yoshida, T., Yokochi, T., Nishiyama, Y. and Kimura, Y. (2002) Olfactory receptor neurons prevent dissemination of neurovirulent influenza A virus into the brain by undergoing virus-induced apoptosis. J. Gen. Virol. 83, 2109–2116.
5 Claeys, S., de Belder, T., Holtappels, G., Gevaert, P., Verhasselt, B., van Cauwenberge, P. and Bachert, C. (2003) Human beta-defensins and toll-like receptors in the upper airway. Allergy 58, 748–753.
6 Suzuki, Y., Takeda, M. and Farbman, A. I. (1996) Supporting cells as phagocytes in the olfactory epithelium after bulbectomy. J. Comp. Neurol. 376, 509–517.
7 Vincent, A. J., Choi-Lundberg, D. L., Harris, J. A., West, A. K. and Chuah, M. I. (2007) Bacteria and PAMPs activate NFκB and Gro production in a subset of olfactory ensheathing cells and astrocytes but not in Schwann cells. Glia 55, 905–916.
8 Vincent, A. J., Taylor, J. M., Choi-Lundberg, D. L., West, A. K. and Chuah, M. I. (2005) Genetic expression profile of olfactory ensheathing cells is distinct from that of Schwann cells and astrocytes. Glia 51, 132–147.
9 Lech, K. and Brent, R. (1992) Escherichia coli, plasmids, and bacteriophages. In: Short Protocols in Molecular Biology, pp. 1–3–1–52, Ausubel, F. M., Brent, R., Kingston, R. E., Moore, D. D., Seidman, J. G., Smith, J. A., Struhl, K. (eds.), Wiley, New York.
10 Chung, R. S., Holloway, A. F., Eckhardt, B. L., Harris, J. A., Vickers, J. C., Chuah, M. I. and West, A. K. (2002) Sheep have an unusual variant of the brain-specific metallothionein, metallothionein-III. Biochem J 365, 323–328.
11 Holtzmann, E. (1989) Lysosomes. Plenum Press, New York.
12 Luzio, J. P., Mullock, B. M., Pryor, P. R., Lindsay, M. R., James, D. E. and Piper, R. C. (2001) Relationship between endosomes and lysosomes. Biochem. Soc. Trans. 29, 476–480.
13 Tennent, R. and Chuah, M. I. (1996) Ultrastructural study of ensheathing cells in early development of olfactory axons. Brain Res. Dev. Brain Res. 95, 135–139.
14 Chuah, M. I. and Au, C. (1991) Olfactory Schwann cells are derived from precursor cells in the olfactory epithelium. J. Neurosci. Res. 29, 172–180.
15 Doucette, R. (1989) Development of the nerve fiber layer in the olfactory bulb of mouse embryos. J. Comp. Neurol. 285, 514–527.
16 Liu, K. L., Chuah, M. I. and Lee, K. K. (1995) Soluble factors from the olfactory bulb attract olfactory Schwann cells. J. Neurosci. 15, 990–1000.
17 Windus, L. C., Claxton, C., Allen, C. L., Key, B. and St John, J. A. (2007) Motile membrane protrusions regulate cell-cell adhesion and migration of olfactory ensheathing glia. Glia 55, 1708–1719.
18 Chuah, M. I., Tennent, R. and Jacobs, I. (1995) Response of olfactory Schwann cells to intranasal zinc sulfate irrigation. J. Neurosci. Res. 42, 470–478.
19 Li, Y., Field, P. M. and Raisman, G. (2005) Olfactory ensheathing cells and olfactory nerve fibroblasts maintain continuous open channels for regrowth of olfactory nerve fibres. Glia 52, 245–251.
20 Pellier, V., Saucier, D., Oestreicher, A. B. and Astic, L. (1996) Ultrastructural and cytochemical identification of apoptotic cell death accompanying development of the fetal rat olfactory nerve layer. Anat. Embryol. (Berl.) 194, 99–109.
21 Wewetzer, K., Kern, N., Ebel, C., Radtke, C. and Brandes, G. (2005) Phagocytosis of O4+ axonal fragments *in vitro* by p75-neonatal rat olfactory ensheathing cells. Glia 49, 577–587.
22 Brogden, K. A., Ackermann, M., McCray, P. B. Jr. and Tack, B. F. (2003) Antimicrobial peptides in animals and their role in host defences. Int. J. Antimicrob. Agents 22, 465–478.
23 Zasloff, M. (2002) Antimicrobial peptides of multicellular organisms. Nature 415, 389–395.
24 Izadpanah, A. and Gallo, R. L. (2005) Antimicrobial peptides. J. Am. Acad. Dermatol. 52, 381–390; quiz 391–2.
25 Ubink, R. and Hökfelt, T. (2000) Expression of neuropeptide Y in olfactory ensheathing cells during prenatal development. J. Comp. Neurol. 423, 13–25.
26 Vincent, A. J., West, A. K. and Chuah, M. I. (2005) Morphological and functional plasticity of olfactory ensheathing cells. J. Neurocytol. 34, 65–80.
27 Vouldoukis, I., Shai, Y., Nicolas, P. and Mor, A. (1996) Broad spectrum antibiotic activity of the skin-PYY. FEBS Lett. 380, 237–240.
28 Hansen, C. J., Burnell, K. K. and Brogden, K. A. (2006) Antimicrobial activity of Substance P and Neuropeptide Y against laboratory strains of bacteria and oral microorganisms. J. Neuroimmunol. 177, 215–218.
29 Getchell, M. L. and Getchell, T. V. (1991) Immunohistochemical localization of components of the immune barrier in the olfactory mucosae of salamanders and rats. Anat. Rec. 231, 358–374.
30 Ibrahim, H. R., Yamada, M., Matsushita, K., Kobayashi, K. and Kato, A. (1994) Enhanced bactericidal action of lysozyme to *Escherichia coli* by inserting a hydrophobic pentapeptide into its C terminus. J. Biol. Chem. 269, 5059–5063.
31 Harris, J. A., Ruitenberg, M. J., West, A. K. and Chuah, M. I. (2008) Inducible production of nitric oxide by olfactory ensheathing cells in response to bacteria. Proc. Aust. Neurosci. Soc. 18, 64.